



**HAL**  
open science

## Fretting-corrosion behavior on dental implant connection in human saliva

Pascale Corne, Pascal de March, Franck Cleymand, Jean Geringer

► **To cite this version:**

Pascale Corne, Pascal de March, Franck Cleymand, Jean Geringer. Fretting-corrosion behavior on dental implant connection in human saliva. *Journal of the mechanical behavior of biomedical materials*, 2019, 94, pp.86-92. 10.1016/j.jmbbm.2019.02.025 . hal-03194105

**HAL Id: hal-03194105**

**<https://hal.science/hal-03194105>**

Submitted on 22 Oct 2021

**HAL** is a multi-disciplinary open access archive for the deposit and dissemination of scientific research documents, whether they are published or not. The documents may come from teaching and research institutions in France or abroad, or from public or private research centers.

L'archive ouverte pluridisciplinaire **HAL**, est destinée au dépôt et à la diffusion de documents scientifiques de niveau recherche, publiés ou non, émanant des établissements d'enseignement et de recherche français ou étrangers, des laboratoires publics ou privés.



Distributed under a Creative Commons Attribution - NonCommercial 4.0 International License

Fretting-corrosion behavior on dental implant connection in human saliva

AUTHOR NAMES AND AFFILIATIONS:

Pascale CORNE, DDS

Associate Professor, Department of Prosthodontics, university of Lorraine, Nancy School  
Dentistry, Nancy Cedex, France

Research group « DOLPHIN, Nanomaterials for life, department N2EV »

Pascal DE MARCH, DDS, Ph.D

Associate Professor, Department of prosthodontics, University of Lorraine, Nancy school  
Dentistry, Nancy Cedex, France

Research group « DOLPHIN, Nanomaterials for life, department N2EV »

UMR7198 CNRS

Franck CLEYMAND, PhD

Assistant Professor

Research group « DOLPHIN, Nanomaterials for life, department  
N2EV »

Jean GERINGER, Ph.D

Assistant Professor, Mines Saint-Etienne, CIS, B2M, UMR, INSERM U1059, Saint-Etienne,  
France

Research group « Centre ingénierie et santé »

## ABSTRACT:

Fretting-corrosion has been pointed out as failure mechanism in dental implants between the implant part and the abutment. Depending on countries, surgical habits, 4 combinations of materials, are well used. The behaviour of fretting corrosion of these four combinations of materials have been highlighted: pure titanium (Ti-grade 4) against titanium alloy (Ti-6Al-4V); titanium alloy (Ti-6Al-4V); against titanium alloy (Ti-6Al-4V); pure titanium against zirconia stabilized with Ytria (Y-TZP) and titanium alloy (Ti-6Al-4V) against zirconia (Y-TZP).

Around 100MPa of contact pressure, approx. the maximal mechanical stresses in dental assembly, after 16 hours of fretting corrosion ( $\pm 40\mu\text{m}$ , displacement) solicitations in Human saliva, the best assembly is Ti material (pure titanium-grade 4) against zirconia in terms of mechanical and electrochemical degradations. The electrochemical behavior has been investigated: the OCP, open circuit potential, is recovering its initial value even during fretting corrosion solicitations, Ti or Ti-6Al-4V against zirconia stabilized with Ytria (Y-TZP), outlier result bur realistic. Some Tribological Transformed Structures on titanium material have been isolated as stir welding effect, STEM observations. Some transfer of zirconia through titanium material has been identified. Ti vs. Y-TZP clearly appears as the best performance couple under fretting corrosion conditions in human saliva. Lastly, some debris due to fretting corrosion have been isolated.

## KEYWORDS:

Dental implant; Human saliva; Fretting-corrosion; Titanium alloys, Y-TZP.

TEXT:

## **1.Introduction**

The dental implant is a common treatment in dentistry. Patients and practitioners would that the dental implant lifetime would be beyond twenty years due to patient issues and health issues (costs, etc.). Unfortunately, the usual biomaterials undergo some damages over the time and this expectation is sometimes follow-up by a failure. Using dental implants dedicated to prosthetic rehabilitation is a usual and successful treatment option (Eliasson et al., 2006; Romeo and Storelli, 2012). Unfortunately, some complications are occurring like osseointegration failures, mechanical degradations or components fractures. Many couples of materials, the complex oral environment (presence of bacteria, acidic or basic fluid, etc.) and the mechanical stresses due to occlusion, mastication and parafunctional habits, are some parameters that may explain these complications. The implant connection is subjected to micro-movements caused by chewing phase, the stresses of the oral environment and some combinations of materials with different mechanical properties (Vieira et al., 2006). This phenomenon worsens even more when the tightening torque is not accurate (Gratton et al., 2001).

Due to the small movements, order of magnitude of few microns, that take place between the elements involved in the mechanical contact, wear phenomenon in dental implant connection involves tribocorrosion or fretting-corrosion studies (Apaza-Bedoya et al., 2017; Mathew et al., 2014; Revathi et al., 2017; Rodrigues et al., 2013; Souza et al., 2012).

Branemark et al. (1983) showed that titanium material is the best material ever to use as implant, i.e. as biomaterial in dental area replacement. It is worth noting that titanium, Ti, or titanium alloy, Ti-6Al-4V, are nowadays well used as orthopedic implants due to their

mechanical properties, moderate density and outstanding biocompatibility compared to other metals. Moreover Ti-6Al-4V, metallic alloy, got some benefits, in terms of Ultimate Tensile Strength (UTS), compared to pure titanium. Furthermore, the titanium alloy, Ti-6Al4V, highlights some additional benefits in terms of corrosion resistance: breakdown potential, corrosion rate, degradation by pitting and crevice corrosion (Solar et al., 1974; Steinemann, 1980).

Recently the authors, Shemtov and Rittel (2015), highlighted that implants retrieval from oral cavity due to progressive bone loss, 60% presented some cracks and total embrittlement. One might notice that Ti-6Al-4V (grade5, Ultimate Tensile Strength, UTS, from 897 to 1205 MPa [14]) alloy that highlights a higher ultimate tensile strength than the one related to pure titanium (grade 4, UTS from 550 to 640 MPa (Cardarelli, 2008)), has the best crack resistance (Shemtov-Yona and Rittel, 2015). The tribological behavior between implant, screw and abutment (dental assembly) is a fruitful approach in order to understand wear mechanisms in implant assembly.

The wide variety of parameters that determine the behavior of the tribological system under these conditions is particularly complex to manage. Several authors (Celis et al., 2006; Fouvry and Kapsa, 2001; Fouvry et al., 1995, 1996, 1997, 2003, 2007; Geringer et al., 2013; Mathew et al., 2012, 2014; Mischler, 2008; Mischler and Munoz, 2018; Mischler and Ponthiaux, 2001; Mischler et al., 1993a, 1993b; Ponthiaux et al., 2004) have been working on this theme and helped to understand the behavior of materials under fretting-corrosion conditions. They have studied the mechanisms taken into account for fretting-corrosion and highlighted the formation of debris that can explain some implants failure by chronic inflammatory reaction. Previous studies have been investigated in standardized solutions (Ringer solution, Hank solution, bovine serum) whose compositions differ from human saliva.

Objectives:

The tribocorrosion of pure titanium, titanium alloy and zirconia material, under fretting corrosion, friction under small relative displacements, in contact with human saliva solutions, will be investigated in order to determine: what is the best couple of materials under fretting-corrosion conditions close to human mouth usage?

## **2. Materials & Methods**

### 2.1 Materials

The investigated materials included pure titanium (Ti-grade 4) like implant or abutment; Titanium alloy (Ti-6Al-4V-grade 5), like implant, abutment or screw; and Yttria-Tetragonal Zirconia Phase (Y-TZP), like abutment. The pure titanium, grade 4, and titanium alloy, grade 5 (Carpenter™, Philadelphia, USA) are manufactured by Carpenter™ (Philadelphia, USA). The Y-TZP material with no-treatment, original color, is distributed by Euromax™ (Monaco, France). No either modification after sintering process was conducted. This material has not been polished in order to avoid any particle insertion from polishing liquid in the bulk material.

Each metallic material has been polished, 1 rectangular face, down to Sa value of 100nm, except Y-TZP. These others faces were gluing with Zircalloy plates and they were varnished in order to insulate the metallic faces from any contact with solution except the fretting-corrosion surface. To allow the formation of a stable and reproducible surface film on the test sample, they were stored 24 hours in an oven (atmospheric pressure, 55°C).

The parallelepipedic sample (9x9x15mm) were in pure Titanium (Ti) or in Ti-6Al-4V. The cylindrical sample were in Ti-6Al-4V (length of 15mm and radius of curvature of 10mm) or Y-TZP (length of 10mm and radius of curvature of 10 mm).

## 2.2 Solution

The investigated solution was conducted in non-stimulated human saliva, i.e. rest saliva. The collect of saliva was practiced, between meals, thanks to salivary cottons placed under the tongue for 5 to 10 minutes thanks to 40 persons ( $22 \pm 2$  years old according to AMM organization through Helsinki declaration). This protocol was repeated several times till getting 200 mL. After, the salivary cottons were pressed thanks to plastic syringe and preserved in freezer. The saliva was gingerly tempered at room temperature (near  $20 \pm 1$  °C) before experiment. The composition was not controlled; one may consider that the salts and proteins concentrations are so close to the actual case (Quintana et al., 2009). The variability is widespread, especially according to Human saliva composition. One of the factor is the time of the day (Neyraud et al., 2012) and it was strictly chosen constant, 10:00am, during the collecting phase ( June 20<sup>th</sup>-24<sup>th</sup>, 2016).

## 2.3 Fretting-corrosion device

The friction was cylinder against plan in order to control the contact mechanics. The experiments have been carried out thanks to a tribocorrosimeter, fretting-corrosion machine, developed by Mines Saint-Etienne and TA instruments™, Company (New Castle, USA) using an electromagnetic motor. A typical fretting-corrosion test was 16 hours of duration, i.e. 57,600 cycles (1s is 1 cycle). The applied normal load, P, was of 127.5 N or 85 N, it is corresponding to the contact pressure (approx. 80 MPa) estimated on the abutment/implant interface by finite element modelling (Ramos Verri, 2015). The sinusoidal amplitude of micro-displacement was  $\pm 40$   $\mu\text{m}$ . As mentioned above, the frequency was of 1 Hz.

*Figure 1: Fretting-corrosion device*

One paid attention on the compliance of the fretting corrosion device that was maintained constant for all tests (Pellier et al., 2011; Kim et al., 2012; Geringer et al., 2013, 2014).

## 2.4 Electrochemical conditions

About Open Circuit Potential (OCP) measurements and the applied cathodic potential, a PARSTAT 2263 potentiostat with two-electrodes for OCP and three-electrodes for applied potential setup have been used. The working electrode was metallic sample, Ti or Ti-6Al-4V. The counter electrode was a platinum wire. The reference electrode was a Saturated Calomel Electrode (SCE,  $E = +242\text{mV/SHE}$ ) at  $T=22^\circ\text{C}$ . A typical electrochemical sequence has been applied from (Celis et al., 2006). The sequence was as following:

1- cathodic polarization ( $-1\text{V/SCE}$ ) during 5 minutes in order to stabilize the oxides formation;

2- OCP phase during 1 hour in order promote the adsorption/desorption equilibrium and an Electrochemical Impedance Spectroscopy sequence (stationary conditions, from  $10^5\text{ Hz}$  to  $10^{-2}\text{ Hz}$ ), without fretting;

Starting fretting during 16 hours

3- OCP measurement during 20 mins;

4- EIS sequence, approx.10 minutes (from  $10^5\text{ Hz}$  to  $10^{-1}\text{ Hz}$ );

33/35 sequences

Stopping fretting

5- OCP measurement, rest OCP.

Due to samples dimensions, the contact surface was of 0.9cm<sup>2</sup>.

The analysis of electrical equivalent circuit was carried out thanks to EC lab software (Bio-Logic Science Instrument™, Seyssinet-Pariset, France). The results will be published in further article.

## 2.5 Surface analysis

The 3D roughness parameters, the total wear volume and the wear track area profile were carried out with Wyko NT9100 (Bruker Nanoscope™, Massachusetts, USA) optical profilometer. Measurements were carried out on five lengths of 1.1 mm and the total wear volume was thus extrapolated for the total wear track on one metallic sample per experiment. Measuring the wear volume on zirconia was unreachable. No wear has been acquired.

The scanning electron microscopy was performed thanks to JEOL™ 6400 (JEOL™, Tokyo, Japan), JEOL™ 6500 FEG (Field Emission Gun) and Quanta FEI™ 650 FEG (FEI™, Oregon, United States) with accelerating voltage between 10 to 15 kV.

The surface morphology and the debris were analyzed by using a Scanning Electron Microscopy (SEM), Zeiss™ Supra 55 (Zeiss™, Oberkochen, Germany). The fretting area was analyzed by using Transmission Electron Microscopy (TEM/STEM), JEOL-ARM200F cold FEG (JEOL™, Tokyo, Japan) 200 kV equipped with probe and image correctors. The thin blade (foil) was performed thanks to Focused Ion Beam, Helios Nanolab 600i. Finally EDS analyses were performed using Centurio spectrometer (ThermoFischer Scientific™, Massachusetts, USA).

### 3.Results

In this work, one may focus on the Open Circuit Potential evolution, phases 2-3&5, part 2.4.

#### 3.1 Open Circuit Potential

During every fretting corrosion experiment, the Open Circuit Potential has been monitored. The Figure 2 shows the OCP evolution related to 4 couples of the four tested materials: Ti-6Al-4V/Ti-6Al-4V; Ti-6Al-4V/Ti; Ti-6Al-4V/Y-TZP; Ti/Y-TZP.

*Figure 2: OCP evolution of the metallic samples, couples Ti-6Al-4V/Y-TZP; Ti/Y-TZP, of the Ti-6Al-4V and the Ti respectively Ti-6Al-4V/Ti-6Al-4V and Ti/Ti-6Al-4V couples of materials. Unit: V vs. SCE reference electrode.*

The OCP evolution is slightly usual: decreasing when the fretting is starting and the OCP is recovering closely its initial value when the fretting stopped.

#### 3.2 Tribological analysis

First of all, the dissipated energy is the area of the tangential load vs. imposed displacement. The cumulated dissipated energy is the sum of each monitored dissipated energy, every second. The wear rate is calculated from the wear volume, the missing material after friction according to a reference plane. It is normalized according to the sliding distance and the

applied normal load. The Figure 3 shows a typical wear track area of Ti-6Al-4V material, 3b) and a fretting log (projection) of the displacement according to tangential load.

*Figure 3: a) Typical wear track area of a Ti-6Al-4V sample; b) Displacement vs. Tangential load, Ti-6Al-4V/Y-TZP contact, green: beginning of the test, blue: middle of the test, red: end of the fretting corrosion test.*

The Figure 4 shows the evolution of the wear rate according to the cumulated dissipated energy.

*Figure 4: Wear rate ( $\text{mm}^3/\text{N.m}$ ) vs. Cumulated dissipated energy (mJ), 4 couples of materials.*

The combination of Ti/Y-TZP materials does highlight the best promising outlook according to the tribological performances, lowest wear rate and lowest dissipated energy.

### 3.3 Wear track area

From some references (Büscher et al., 2005; Pourzal et al., 2009, 2011; Rainforth et al., 2012; Wimmer et al., 2010) related to some investigated couples, some stresses coming from the fretting corrosion solicitations were triggering some microstructural changes from the top surfaces till the bulk materials. This layer is well known as the tribological transformed structure (TTS). The thickness may be considered around 3-4  $\mu\text{m}$ . The stresses that were generated during the fretting solicitations were involving some changes of the material

structure, some grains refinement as an example. Moreover, the dissipated energy, during friction, is dedicated to produce some debris. Some high resolution SEM, Scanning Electron Microscope, images emphasize this behavior.

One might suggest to start by the two metallic combinations: Ti-6Al-4V/Ti-6Al-4V and the Ti/Ti-6Al-4V.

### 3.3.1 Metallic combinations: Ti-6Al-4V/Ti-6Al-4V and Ti/Ti-6Al-4V.

The titanium alloy/titanium alloy combination exhibits a typical behavior. The Figure 5) is showing: a) the total wear track area and b) a crack beneath the top surface provided by observing a cross section inside the wear track area.

*Figure 5: a) the wear track area corresponding to Ti-6Al-4V/Ti-6Al-4V; b) a cross section observation practiced inside the wear track area.*

Another interesting point is related to the presence of a third body layer compacted on some parts of the wear track area, Figure 6. The thickness of the third body layer on Figure 6a) is about 1 $\mu$ m. It is worth noting that some metallic debris get an average diameter lower than 1 $\mu$ m.

*Figure 6: a) the wear track area corresponding to Ti-6Al-4V/Ti-6Al-4V; b) a cross section observation practiced inside the wear track area.*

This compacted layer is promising some tribological benefits during the friction phase; however, concerning the biocompatibility one may suggest the toxicity of this kind of particles. The Figure 6b) is assessing the third body compaction. One may suggest that the adherence of this layer is efficient. After the polishing step, the debris were adherent on the metallic sample. Even the friction promotes the delamination, a compacted third debris layer is agglomerated on the top surface. The Figure 7 shows the image corresponding to a lamella issued from TEM microtome. Some dislocations are generated and the pristine microstructure is completely damaged. At that time, it is interesting to compare the pattern of figure 7a) with the one related to the titanium alloy that was rubbed against Y-TZP material. The pristine grains are well defined. No microstructure has been modified on the contrary of Ti-6Al-4V/Ti-6Al-4V. One may consider that due to adherence between Ti-6Al-4V/Ti-6Al-4V, the grain structure is altered and many dislocations have been created, 'black cloud' on the Figure 7a.

*Figure 7: a) TEM analysis in the wear track area Ti-6Al-4V/Ti-6Al-4V, STEM HAADF; b) TEM analysis in the wear track area Ti-6Al-4V/Y-TZP, STEM HAADF*

### 3.3.2 Metal/Ceramic combinations: Ti-6Al-4V/Y-TZP and Ti/ Y-TZP against Y-TZP.

The counter material is quite ceramic material, Y-TZP in this section. The Figure 8 is showing some small particles, debris, in the wear track area of the Ti-6Al-4V. The small particles are slightly, it might be some zirconia particles. The most relevant point is the size, i.e. lower than 1µm, roughly few 100nm. No zirconia material has been found inside the Ti-6Al-4V: it means that there is no mixing process between both materials on the contrary of

metal/metal contact. Thanks to Figure 8b), some grains refinement was occurring by comparison some grains on the top, TTS, and some grains from the down part, bulk material.

*Figure 8: a) SEM image on the wear track area; b) TEM analysis under the wear track area of Ti-6Al-4V sample in the contact with Y-TZP*

The Figure 9 is quite informative. On the contrary of Ti-6Al-4V, the Ti top surface was modified thanks to fretting corrosion experiments. The grain size did change, refinement, and the most relevant is, on the Figure 9b), some ceramic material is inserted in the TTS of the titanium sample.

*Figure 9: a) TEM analysis in the wear track area of Ti sample in the contact with Y-TZP, STEM HAADF; b) From the same image, EDS: the pink material is Zirconium.*

### 3.4 Discussion

About OCP evolution, at the starting point of fretting (friction), the OCP was decreasing. As a matter of fact, the passive film is destroyed due to friction, rubbing, and the open circuit potential is decreasing due to charges production (ions). It is worth noting that the more drastic OCP drop is related to Ti-6Al-4V/Ti-6Al-4V, figure [2]. The passive film of this alloy is well classified, after friction, as non-protective (Galliano et al., 2001). During the rubbing phase, the OCP is slightly constant without any recovering process. Except Ti/Y-TZP case, the OCP is recovering its initial value (the one before fretting), it is worth noting that it is

happening during the fretting phase. Thus, both hypotheses may be ongoing: the titanium oxides layer may be recovered and the zirconia may play the role of coating when some zirconia debris are slightly recovering the titanium metal, avoiding an anodic current. The Figure 9 is a clue of this assertion. To summarize concerning the OCP evolution, Ti/Y-TZP combination highlights a kind of protective effect during the fretting corrosion phase.

Both Figures, Figures 7a and 7b, are related to stir welding modified structure on Ti-6Al-4V (Fall et al., 2016). The contact stresses are lower than the ones evoked in the Fall et al. reference. The temperature was around 1000°C in the publication, not the case in this study, it is in solution, i.e. room temperature. About the contact stresses and the rotation speed, comparing the order of magnitude may be relevant: FSW case (Arora et al., 2012), it is a question of 40MPa and 3,5mm/s and in the investigated study, it is a question of 80 MPa and 0,008mm/s. It makes sense that the depth of the TTS (fretting corrosion-85N-80µm/s) is roughly 1000 times lower than the one of (stir welding-3000N-3.5mm/s).

Notwithstanding the experimental conditions were drastically different; the morphology related to the Tribological Transformed Structure is similar. Concerning the FSW, friction stir welding, between Titanium alloy against titanium alloy, the affected zone, depth, was around few millimeters. Concerning the affected zone of our study, the Ti-6Al-4V was modified due to fretting corrosion on a roughly depth of few micrometers, Figure 7. Three orders of magnitude are concerned between both cases but the morphology is quite the same. The Figure 9 is showing some MET observations, some lamella and information from EDS. It is worth noting that pure Ti sample is containing some aluminium metal in the TTS. It is the clue to assess that there is some metallic transfer during fretting corrosion from Ti-6Al-4V to Ti. It might call a kind of 'fretting stir welding'.

After fretting corrosion, there is a kind of welding phase by mixing materials. Some zirconia was compacted on the top surface of Ti material. On Ti-6Al-4V, this insertion was

not highlighted. Under stresses, the pure titanium is well accepted the zirconia material as third body, the tribological transformed structure is constituted by mixing both materials in contact, on the contrary of Ti-6Al-4V material. From the physical point of view, one may compare the thermal conductivity and the elongation related to grade 4 and grade 5.

#### Physical properties and diffusion of material

	Unit	Grade 4	Grade 5
Thermal Conductivity	W/m.k	17.3	6.6
Elongation	%	23	18

*Table 1: Thermal conductivity (W/m.K) and elongation (%) of pure titanium, grade 4 and titanium alloy, grade 5 (www.ife.no)*

Because of the higher elongation and the thermal conductivity, Ti grade 4, pure titanium may get the ability by transferring more energy in the bulk material than titanium alloy, grade 5.

Some debris are from different shapes and sizes due to fretting degradations. From SEM image, Figure 8a), their size is from micrometrical scale till dozens of nanometers. By keeping in mind that gingiva fibroblast diameter is of 30  $\mu\text{m}$ , the nanometric scale of debris may encounter some issues about the bone and gingival remodeling. These debris may enhance the phagocytosis by fibroblast and disrupted the usual cells functioning, leading enjoy to apoptosis. This debris misfit was well described in the literature (Mathew et al., 2014; Revathi et al., 2017; Sridhar et al., 2016). Some inflammation, some weird deceleration around implants, was identified around some implants, i.e. allergy (Chaturvedi, 2009). Moreover, due to debris, the osteoclasts differentiation is promoted; thus, the implant failure is ongoing. It is worth noting most of the time, some implants failures are attributed to the dental plaques (Persson and Renvert, 2014). Due to debris when considering some dental

implants, debris may account for implants failure, more than dental plaque (Apaza-Bedoya et al., 2017).

#### 4. Conclusion

From this study to mimic the in vitro degradation of some dental implant's connections, the pure titanium (grade 4)/Y-TZP assembly is the best one under fretting corrosion solicitations, OCP increase during the fretting phase. Three other combinations were tested: Titanium alloy, Ti-6Al-4V, vs. zirconia (Y-TZP), Ti-6Al-4V/Ti-6Al-4V and Ti-6Al-4V/Ti. The titanium material is well transformed on the top surface. The tribological transformed structure was well characterized on the titanium material. Some transfer of material has been demonstrated: the zirconia material is embedded inside the Ti counterface. This transfer is one key explanation to explain the increase of OCP during fretting (surprising) and the lowest dissipated energy and wear volume, Ti vs. Y-TZP combination.

Some further materials are nowadays investigated. One might notice that Benea et al.(Benea et al., 2015) made some improvements to enhance the durability of Ti-6Al-4V material as dental implant. Some nanotubes were investigated to enhance the electrochemical stability by promoting a promising osseointegration (Alves et al., 2017). The titanium alloy (titanium-tantalum) (Mareci et al., 2009) and Beta phase titanium alloy should present better corrosion resistance than usual titanium alloy, Ti-6Al-4V, some wear resistance (Cordeiro and Barão, 2017; Revathi et al., 2017). In odontology field, these materials may be a good way to develop promising insights.

## References:

Al Jabbari, Y.S., Fournelle, R.A., Zinelis, S., Iacopino, A.M., 2012. Biotribological Behavior of Two Retrieved Implant Abutment Screws after Long-Term Use In Vivo. *Int. J. Oral. Max. Impl.* 27, 1474–1480.

Alves, S.A., Rossi, A.L., Ribeiro, A.R., Toptan, F., Pinto, A.M., Celis, J.-P., Shokuhfar, T., Rocha, L.A., 2017. Tribo-electrochemical behavior of bio-functionalized TiO<sub>2</sub> nanotubes in artificial saliva: Understanding of degradation mechanisms. *Wear.* 384–385, 28–42.

Apaza-Bedoya, K., Tarce, M., Benfatti, C.M., Henriques, B., Mathew, M.T., Teughels, W., Souza, J.C.M., 2017. Synergistic interactions between corrosion and wear at titanium-based dental implant connections: A scoping review. *J. Periodontal. Res.* 52, 946-954.

Arora, A., Mehta, M., De, A., DebRoy, T., 2012. Load bearing capacity of tool pin during friction stir welding. *Int. J. Adv. Manuf. Tech.* 61, 911–920.

Benea, L., Danaila, E., Ponthiaux, P., 2015. Effect of titania anodic formation and hydroxyapatite electrodeposition on electrochemical behaviour of Ti–6Al–4V alloy under fretting conditions for biomedical applications. *Corros. Sci.* 91, 262–271.

Bordin, D., Cavalcanti, I.M.G., Jardim Pimentel, M., Fortulan, C.A., Sotto-Maior, B.S., Del Bel Cury, A.A., da Silva, W.J., 2015. Biofilm and saliva affect the biomechanical behavior of dental implants. *J. Biomech.* 48, 997–1002.

Branemark, P.-I., 1983. Osseointegration and its experimental background. *J. Prosthet. Dent.* 50, 399–410.

Büscher, R., Täger, G., Dudzinski, W., Gleising, B., Wimmer, M.A., Fischer, A., 2005. Subsurface microstructure of metal-on-metal hip joints and its relationship to wear particle generation. *J. Biomed. Mater. Res. B.* 72, 206–214.

Cardarelli, F., 2008. *Materials Handbook, Second ed.* Springer, London.

Celis, J-P., Ponthiaux, P., Wenger, F., 2006. Tribo-corrosion of materials: Interplay between chemical, electrochemical, and mechanical reactivity of surfaces. *Wear.* 261, 939–946.

Chaturvedi, T.P., 2009. An overview of the corrosion aspect of dental implants (titanium and its alloys). *Indian. J. Dent. Res.* 20, 91–98.

Clavel, M., Bompard, P., 2009. *Endommagement et rupture des matériaux 1, First ed.* Lavoisier, Paris.

Cordeiro, J.M., Barão, V., 2017. Is there scientific evidence favoring the substitution of commercially pure titanium with titanium alloys for the manufacture of dental implants? *Mater. Sci. Eng.* 1, 1201–1215.

Eliasson, A., Eriksson, T., Johansson, A., Wennerberg, A., 2006. Fixed Partial Prostheses Supported by 2 or 3 Implants: A Retrospective Study up to 18 Years. *Int. J. Oral. Max. Impl.* 21, 567–574.

Fall, A., Fesharaki, M., Khodabandeh, A., Jahazi, M., Fall, A., Fesharaki, M.H., Khodabandeh, A.R., Jahazi, M., 2016. Tool Wear Characteristics and Effect on Microstructure in Ti-6Al-4V Friction Stir Welded Joints. *Metals-Basel*. 6, 275.

Fouvry, S., Kapsa, P., 2001. An energy description of hard coating wear mechanisms. *Surf. Coat. Tech.* 138, 141–148.

Fouvry, S., Kapsa, P., Vincent, L., 1995. Analysis of sliding behaviour for fretting loadings: determination of transition criteria. *Wear*. 185, 35–46.

Fouvry, S., Kapsa, P., Vincent, L., 1996. Quantification of fretting damage. *Wear*. 200, 186–205.

Fouvry, S., Kapsa, P., Zahouani, H., Vincent, L., 1997. Wear analysis in fretting of hard coatings through a dissipated energy concept. *Wear*. 203–204, 393–403.

Fouvry, S., Liskiewicz, T., Kapsa, P., Hannel, S., Sauger, E., 2003. An energy description of wear mechanisms and its applications to oscillating sliding contacts. *Wear*. 255, 287–298.

Fouvry, S., Paulin, C., Liskiewicz, T., 2007. Application of an energy wear approach to quantify fretting contact durability: Introduction of a wear energy capacity concept. *Tribol. Int.* 40, 1428–1440.

Galliano, F., Galvanetto, E., Mischler, S., Landolt, D., 2001. Tribocorrosion behavior of plasma nitrided Ti-6Al-4V alloy in neutral NaCl solution. *Surf. Coat. Tech.* 145, 121–131.

Kim K., Geringer J., 2012, Analysis of energy dissipation in fretting corrosion experiments with materials used as hip prosthesis. *Wear*, 296, 497-503

Geringer, J., Kim, K., Pellier, J., Macdonald, D.D., 2013. Fretting corrosion processes and wear mechanisms in medical implants, in: Yan, Y. (Ed.), *Bio-Tribocorrosion in Biomaterials and Medical Implants*. Woodhead Publishing, Cambridge, pp. 45–73.

Geringer J., Macdonald D.D., 2014, Friction/Fretting-corrosion mechanisms: current trends and outlooks for implants. *Mat. Letters* 134, 152-158

Gratton, D.G., Aquilino, S.A., Stanford, C.M., 2001. Micromotion and dynamic fatigue properties of the dental implant–abutment interface. *J. Prosthet. Dent.* 85, 47–52.

Gurappa, I., 2002. Characterization of different materials for corrosion resistance under simulated body fluid conditions. *Mater. Charac.* 49, 73–79.

Jolivet, J-P., 2016. *De la solution à l'oxyde*, Second ed. Edp Sciences, Paris.

Licausi, M.P., Igual Muñoz, A., Amigó Borrás, V., 2013. Influence of the fabrication process and fluoride content on the tribocorrosion behaviour of Ti6Al4V biomedical alloy in artificial saliva. *J. Mech. Behav. Biomed.* 20, 137–148.

Mareci, D., Chelariu, R., Gordin, D.-M., Ungureanu, G., Gloriant, T., 2009. Comparative corrosion study of Ti-Ta alloys for dental applications. *Acta. Biomater.* 5, 3625–3639.

Mathew, M.T., Barão, V.A., Yuan, J.C.-C., Assunção, W.G., Sukotjo, C., Wimmer, M.A., 2012. What is the role of lipopolysaccharide on the tribocorrosive behavior of titanium? *J. Mech. Behav. Biomed.* 8, 71–85.

Mathew, M.T., Kerwell, S., Lundberg, H.J., Sukotjo, C., Mercuri, L.G., 2014. Tribocorrosion and oral and maxillofacial surgical devices. *Brit. J. Oral. Max. Surg.* 52, 396–400.

Mischler, S., 2008. Triboelectrochemical techniques and interpretation methods in tribocorrosion: A comparative evaluation. *Tribol. Int.* 41, 573–583.

Mischler, S., Munoz, A.I., 2018. Tribocorrosion, in: Wandelt K., *Encyclopedia of interfacial chemistry*. Elsevier, New York, pp 504-514.

Mischler, S., Ponthiaux, P., 2001. A round robin on combined electrochemical and friction tests on alumina/stainless steel contacts in sulphuric acid. *Wear.* 248, 211–225.

Mischler, S., Rosset, E.A., Landolt, D., 1993a. Effect of Corrosion on the Wear Behavior of Passivating Metals in Aqueous Solutions, in: Dowson, D., Taylor, C.M., Childs, T.H.C., Godet, M., Dalmaz, G. (Eds.), *Tribology Series*. Elsevier, New York, pp. 245–253.

Mischler, S., Rosset, E., Stachowiak, G.W., Landolt, D., 1993. Effect of sulphuric acid concentration on the rate of tribocorrosion of iron. *Wear.* 167, 101–108.

Neyraud, E. Palicki, O., Schwartz, C., Nicklaus, S., Feron, G., 2012. Variability of human saliva composition: Possible relationships with fat perception and liking. *Archives of Oral Biology*. 57, 556-566.

Persson, G.R., Renvert, S., 2014. Cluster of bacteria associated with peri-implantitis. *Clin. Implant. Dent. R.* 16, 783–793.

Pellier J., Geringer J., Forest B., 2011. Fretting corrosion between 316LSS and PMMA: influence of ionic strength, protein and electrochemical conditions on material wear. Application to orthopedic implants. *Wear*. 271, 1563-1571.

Ponthiaux, P., Wenger, F., Drees, D., Celis, J.P., 2004. Electrochemical techniques for studying tribocorrosion processes. *Wear*. 256, 459–468.

Pourzal, R., Theissmann, R., Williams, S., Gleising, B., Fisher, J., Fischer, A., 2009. Subsurface changes of a MoM hip implant below different contact zones. *J. Mech. Behav. Biomed.* 2, 186–191.

Pourzal, R., Catelas, I., Theissmann, R., Kaddick, C., Fischer, A., 2011. Characterization of Wear Particles Generated from CoCrMo Alloy under Sliding Wear Conditions. *Wear*. 271, 1658–1666.

Quintana, M., Palicki O., Lucchi G., Ducoroy P., Chambone C., Salles C., Morzel M., 2009. Inter-individual variability of protein patterns in saliva of healthy adults. *Journal of Proteomics*. 72, 822-830

Rainforth, W.M., Zeng, P., Ma, L., Valdez, A.N., Stewart, T., 2012. Dynamic surface microstructural changes during tribological contact that determine the wear behaviour of hip prostheses: metals and ceramics. *Faraday. Discuss.* 156, 41–57.

Ramos Verri F., Ferreira Santiago J., Augusto de Faria Almeida D., Bergamo Brandao de Oliveira G., Eduardo de Souza Batista V., Marques Honorio H., Yoshito Noritomi P., Piza Pellizzer E. 2015. Biomechanical influence of crown-to-implant ratio on stress distribution over internal hexagon short implant: 3-D finite element analysis with statistical test. *J. of Biomech.* 48, 138-145

Revathi, A., Borrás, A.D., Muñoz, A.I., Richard, C., Manivasagam, G., 2017. Degradation mechanisms and future challenges of titanium and its alloys for dental implant applications in oral environment. *Mat. Sci. Eng. C-Mater.* 76, 1354–1368.

Rodrigues, D.C., Valderrama, P., Wilson, T.G., Palmer, K., Thomas, A., Sridhar, S., Adapalli, A., Burbano, M., Wadhvani, C., 2013. Titanium Corrosion Mechanisms in the Oral Environment: A Retrieval Study. *Materials.* 6, 5258–5274.

Romeo, E., Storelli, S., 2012. Systematic review of the survival rate and the biological, technical, and aesthetic complications of fixed dental prostheses with cantilevers on implants reported in longitudinal studies with a mean of 5 years follow-up. *Clin. Implant. Dent. R.* 23, 39–49.

Royhman, D., Dominguez-Benetton, X., Yuan, J.C.-C., Shokuhfar, T., Takoudis, C., Mathew, M.T., Sukotjo, C., 2015. The Role of Nicotine in the Corrosive Behavior of a Ti-6Al-4V Dental Implant. *Clin. Implant. Dent. R.* 17, 352-363.

Ryu, J.J., Shrotriya, P., 2013. Synergistic mechanisms of bio-tribocorrosion in medical implants, in: Yan, Y. (Ed.), *Bio-Tribocorrosion in Biomaterials and Medical Implants*. Woodhead Publishing, Cambridge, pp. 25–46.

Shemtov-Yona, K., Rittel, D., 2015. On the mechanical integrity of retrieved dental implants. *J. Mech. Behav. Biomed.* 49, 290–299.

Solar, R., Pollack, S., Korostoff, E., 1974. Titanium release from implants: a proposed mechanism. *J. Biomed. Mater. Res.* 219–226.

Souza, J.C.M., Barbosa, S.L., Ariza, E., Celis, J.-P., Rocha, L.A., 2012. Simultaneous degradation by corrosion and wear of titanium in artificial saliva containing fluorides. *Wear.* 292–293, 82–88.

Sridhar, S., Abidi, Z., Wilson, T.G., Valderrama, P., Wadhvani, C., Palmer, K., Rodrigues, D.C., 2016. In Vitro Evaluation of the Effects of Multiple Oral Factors on Dental Implants Surfaces. *J. Oral. Implantol.* 42, 248–257.

Steinemann, S., 1980. Corrosion of surgical implants in vivo and in vitro tests, in: Winter, G.D., Leray, J., de Groot, K. (Eds.), *Evaluation of Biomaterials*. John Wiley, New York, pp. 1-34

Vieira, A.C., Ribeiro, A.R., Rocha, L.A., Celis, J.P., 2006. Influence of pH and corrosion inhibitors on the tribocorrosion of titanium in artificial saliva. *Wear*. 261, 994–1001.

Wimmer, M.A., Fischer, A., Büscher, R., Pourzal, R., Sprecher, C., Hauert, R., Jacobs, J.J., 2010. Wear mechanisms in metal-on-metal bearings: the importance of tribochemical reaction layers. *J. Orthop. Res.* 28, 436–443.

Web reference:

[https://www.ife.no/en/ife/departments/materials\\_and\\_corrosion\\_tech/files/facts-and-figures-for-commonly-used-titanium-alloys](https://www.ife.no/en/ife/departments/materials_and_corrosion_tech/files/facts-and-figures-for-commonly-used-titanium-alloys) (accessed 26 september 2018)

Captions:

Figure 1: Fretting-corrosion device

Figure 2: OCP evolution of the metallic samples, couples Ti-6Al-4V/Y-TZP; Ti/Y-TZP, of the Ti-6Al-4V and the Ti respectively Ti-6Al-4V/Ti-6Al-4V and Ti/Ti-6Al-4V couples of materials. Unit: V vs. SCE reference electrode.

Figure 3: a) Typical wear track area of a Ti-6Al-4V sample; b) Displacement vs. Tangential load, Ti-6Al-4V/Y-TZP contact, green: beginning of the test, blue: middle of the test, red: end of the fretting corrosion test.

Figure 4: Wear rate ( $\text{mm}^3/\text{N.m}$ ) vs. Cumulated dissipated energy (mJ), 4 couples of materials.

Figure 5: a) the wear track area corresponding to Ti-6Al-4V/Ti-6Al-4V; b) a cross section observation practiced inside the wear track area.

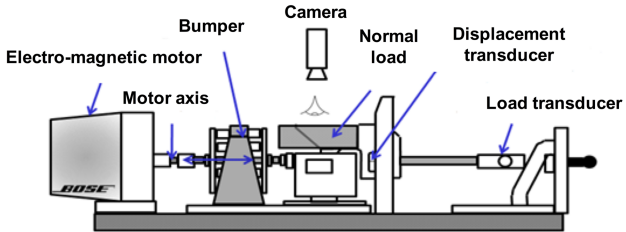
Figure 6: a) the wear track area corresponding to Ti-6Al-4V/Ti-6Al-4V; b) a cross section observation practiced inside the wear track area.

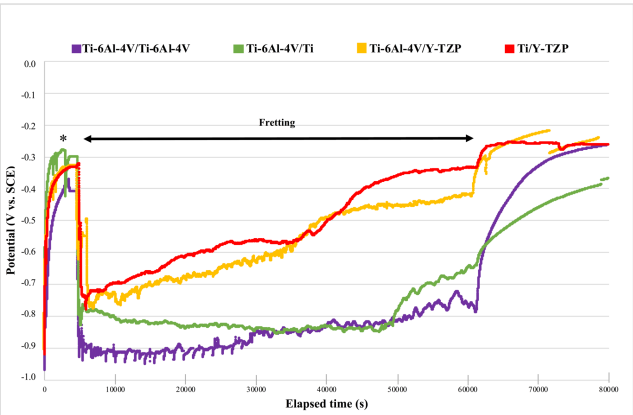
Figure 7: a) TEM analysis in the wear track area Ti-6Al-4V/Ti-6Al-4V, STEM HAADF; b) TEM analysis in the wear track area Ti-6Al-4V/Y-TZP, STEM HAADF

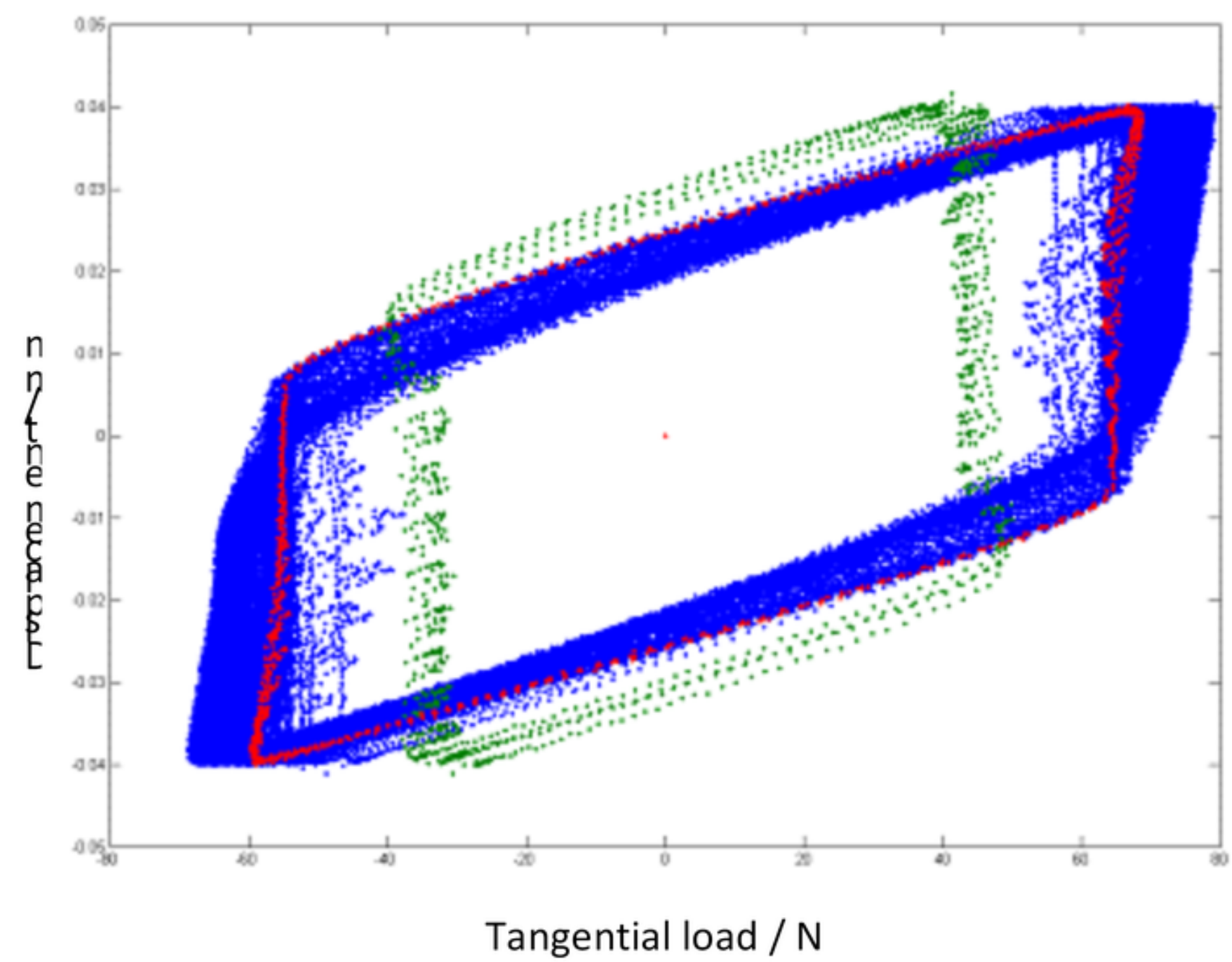
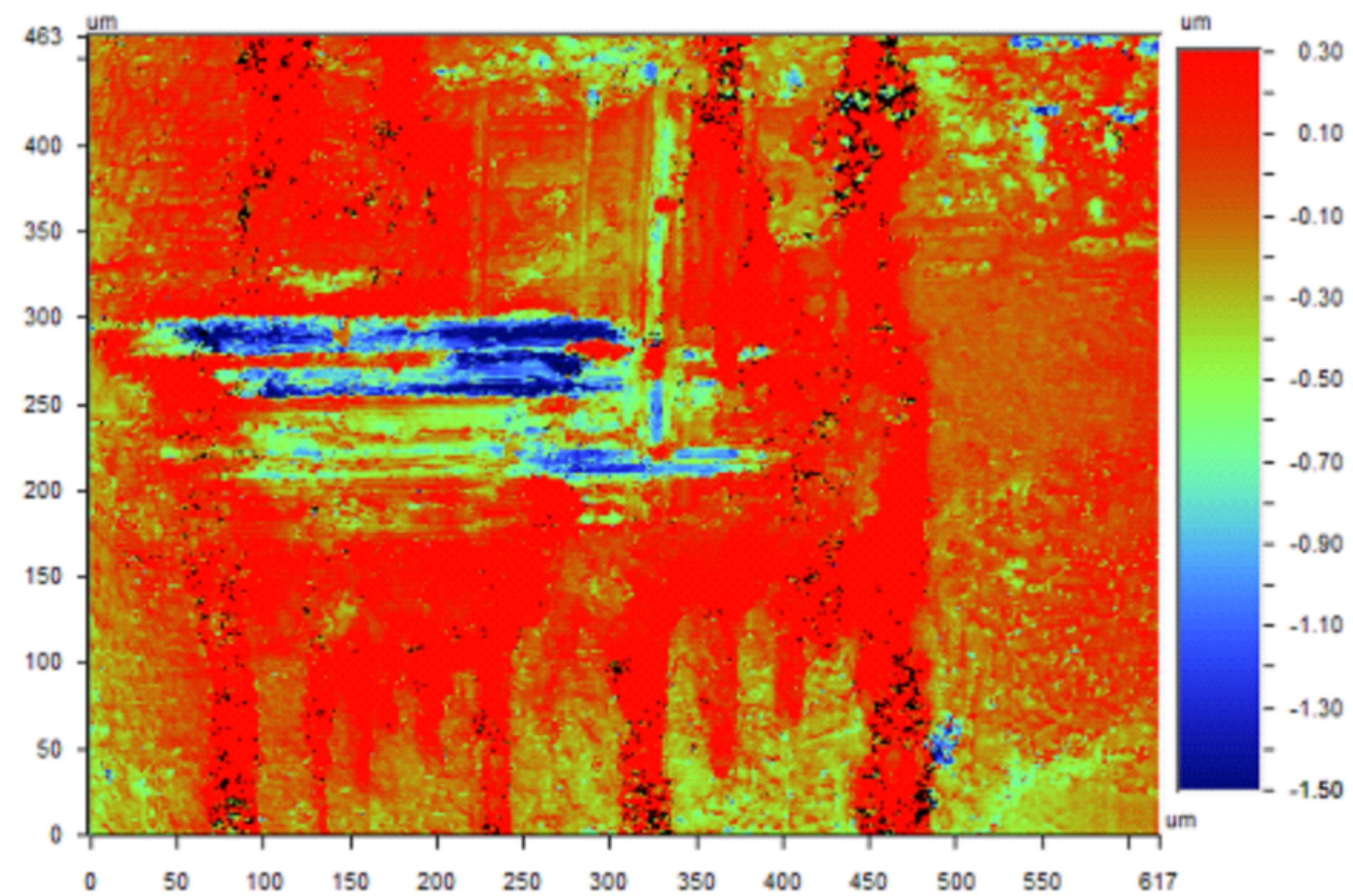
Figure 8: Figure 8: a) SEM image on the wear track area; b) TEM analysis under the wear track area of Ti-6Al-4V sample in the contact with Y-TZP

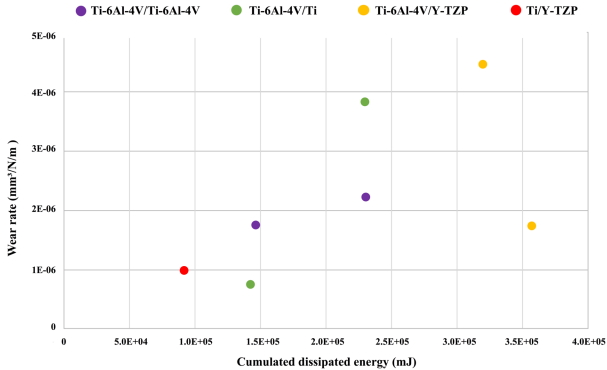
Figure 9: a) TEM analysis in the wear track area of Ti sample in the contact with Y-TZP, STEM HAADF; b) From the same image, EDS: the pink material is Zirconium.

Table 1: Thermal conductivity ( $\text{W/m.K}$ ) and elongation (%) of pure titanium, grade 4 and titanium alloy, grade 5 ([www.ife.no](http://www.ife.no))











20 µm



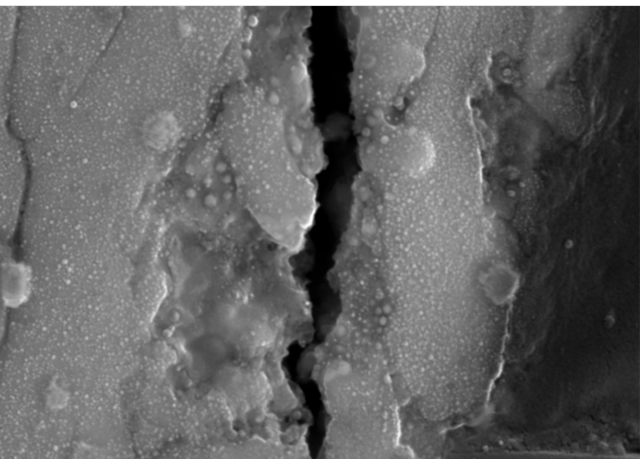
Mag = 599 X  
WD = 14.3 mm

Signal A = SE2  
EHT = 20.00 kV

Date : 25 Aug 2016  
Time : 11:45:53

30 µm





200 nm



Mag = 50.00 K X

WD = 13.4 mm

Signal A = SE2

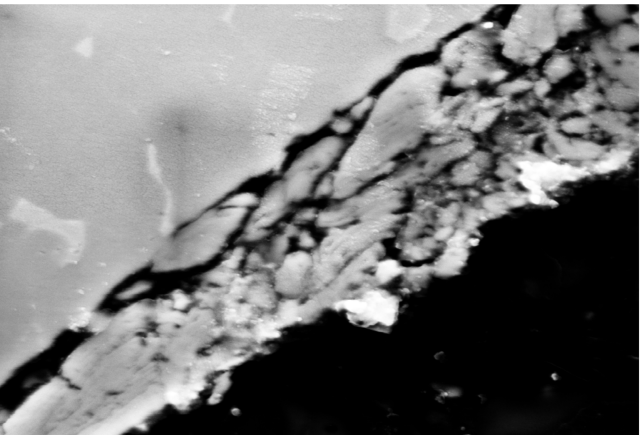
EHT = 20.00 kV

Date :22 Dec 2016

Time :15:36:56



Ecole Nationale  
Supérieure des Mines  
SAINT-ETIENNE

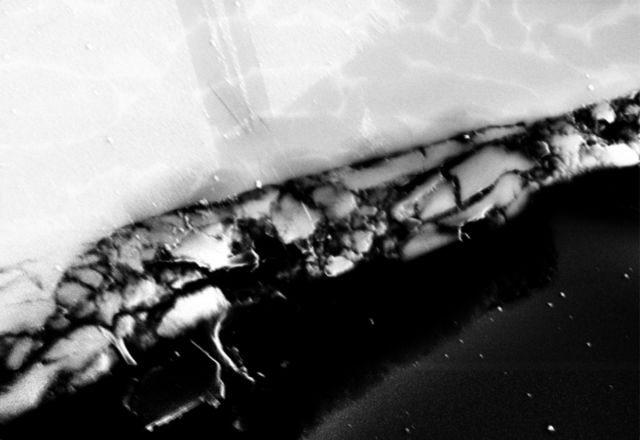


1  $\mu\text{m}$   


Mag = 30.00 K X  
WD = 16.6 mm

Signal A = SE2  
EHT = 10.00 kV

Date :20 Dec 2016  
Time :15:52:54



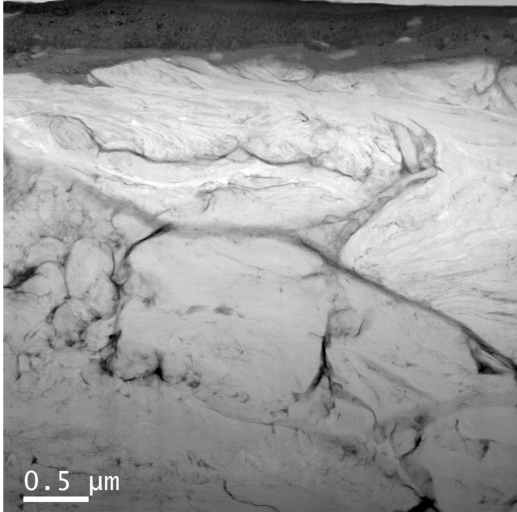
2  $\mu$ m



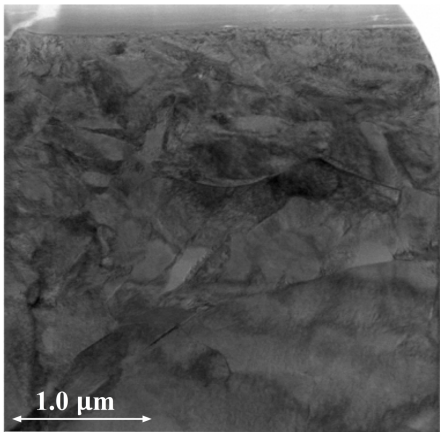
Mag = 11.79 K X  
WD = 16.1 mm

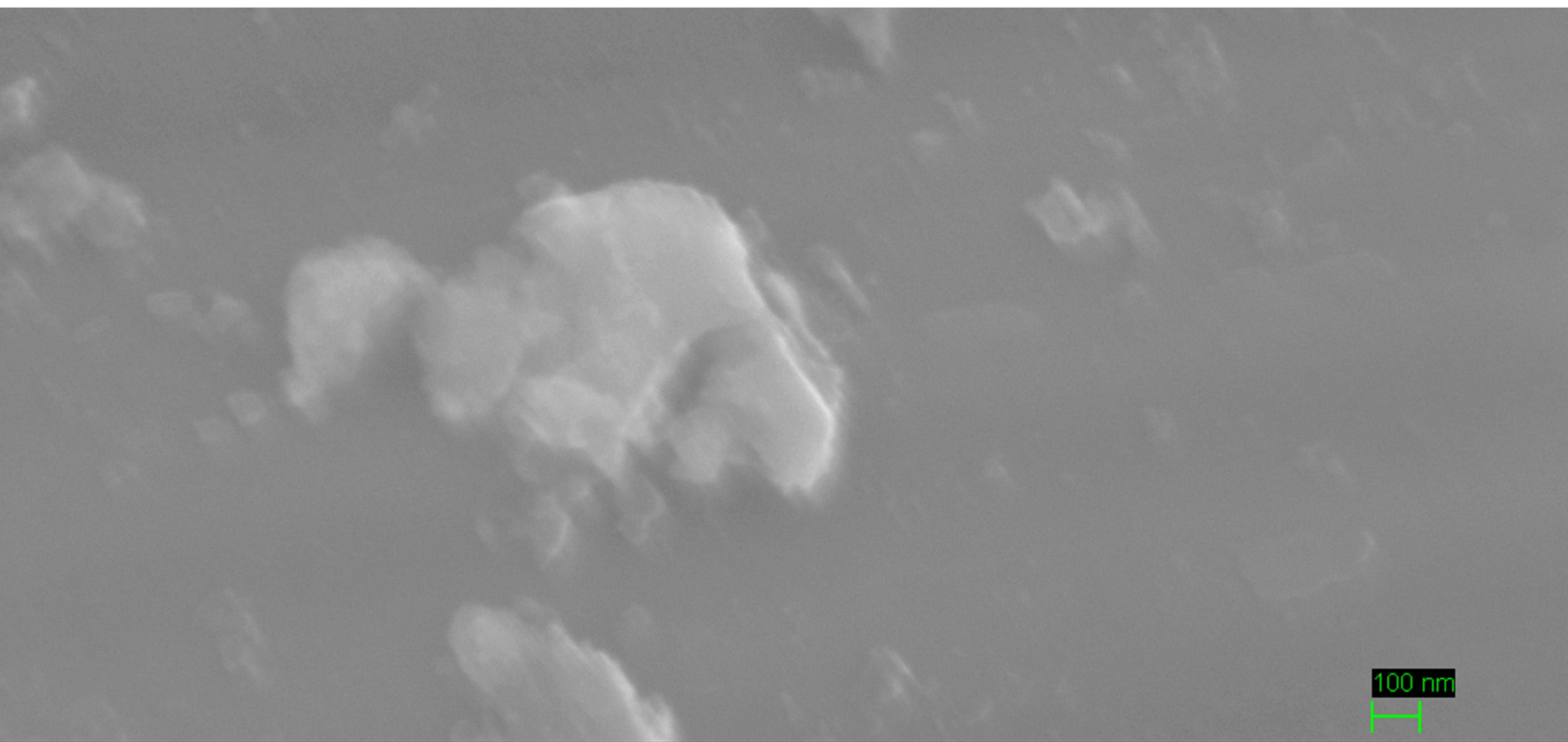
Signal A = SE2  
EHT = 20.00 kV

Date : 19 Dec 2016  
Time : 15:37:08



**SURFACE**





100 nm



100 nm



Mag = 90.00 K X  
WD = 15.1 mm

Signal A = SE2  
EHT = 20.00 kV

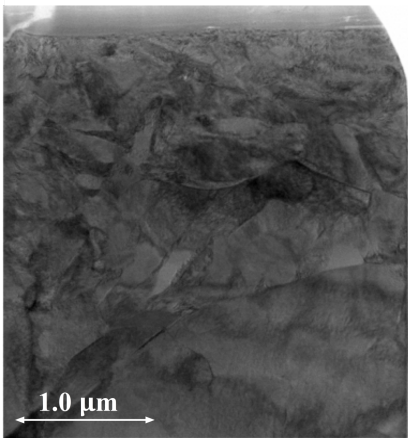
Date :25 Aug 2016  
Time :13:45:09



Ecole Nationale  
Supérieure des Mines  
SAINT-ETIENNE



**SURFACE**



**1.0  $\mu\text{m}$**



